HHS Public Access

Author manuscript

Ann Nucl Med. Author manuscript; available in PMC 2022 December 22.

Published in final edited form as:

Ann Nucl Med. 2019 August ; 33(8): 617–623. doi:10.1007/s12149-019-01371-8.

Improved identification of patients with oligometastatic clear cell renal cell carcinoma with PSMA-targeted ^{18}F-DCFPyL PET/CT

Alexa R. Meyer[1], **Michael A. Carducci**[1,2], **Samuel R. Denmeade**[1,2], **Mark C. Markowski**[2], **Martin G. Pomper**[1,2,3], **Philip M. Pierorazio**[1,2], **Mohamad E. Allaf**[1,2], **Steven P. Rowe**[1,3], **Michael A. Gorin**[1,2,3]

[1]The James Buchanan Brady Urological Institute and Department of Urology, Johns Hopkins University School of Medicine, 600 North Wolfe Street, Park 213, Baltimore, MD 21287, USA

[2]Department of Oncology, Sydney Kimmel Comprehensive Cancer Center, Johns Hopkins University of Medicine, Baltimore, MD, USA

[3]The Russell H. Morgan Department of Radiology and Radiological Science, Johns Hopkins University School of Medicine, Baltimore, MD, USA

Abstract

Objective—Complete surgical resection of metastatic sites has been shown to prolong survival in select patients with oligometastatic RCC. This treatment strategy is dependent upon the accurate characterization of a patient's extent of disease. The objective of this study was to explore the utility of PSMA-targeted ^{18}F-DCFPyL PET/CT in patients with presumed oligometastatic clear cell RCC.

Methods—This is a subset analysis of a prospective study in which patients with RCC were imaged with ^{18}F-DCFPyL PET/CT (ClinicalTrials.gov identifier NCT02687139). In the present analysis, patients with oligometastatic clear cell RCC, defined as ≤ 3 metastatic lesions on conventional imaging, were evaluated. ^{18}F-DCFPyL PET/CT scans were reviewed for sites of disease and compared to conventional imaging.

Results—The final cohort included 14 patients with oligometastatic clear cell RCC. Conventional imaging revealed 21 metastatic lesions and 3 primary tumors. ^{18}F-DCFPyL PET/CT detected 29 sites of metastatic disease and 3 primary tumors. Of the 21 metastatic lesions detected on conventional imaging, 17 (81.0%) had radiotracer uptake. Additionally, all 3 primary tumors had radiotracer uptake. In 4 (28.6%) patients a total of 12 more lesions were identified on ^{18}F-DCFPyL PET/CT than conventional imaging. Notably, 3 (21.4%) patients were no longer considered oligometastatic. The detection rates of conventional imaging and ^{18}F-DCFPyL PET/CT for identifying sites of disease were 66.7% and 88.9%, respectively.

✉Michael A. Gorin, mgorin1@jhmi.edu.

Compliance with ethical standards

Conflict of interest MGP is a co-inventor on a US Patent covering ^{18}F-DCFPyL and as such is entitled to a portion of any licensing fees and royalties generated by this technology. This arrangement has been reviewed and approved by the Johns Hopkins University in accordance with its conflict-of-interest policies. MAG has served as a consultant to Progenics Pharmaceuticals, the licensee of ^{18}F-DCFPyL. SPR, MAG, and MGP have received research support from Progenics Pharmaceuticals.

Conclusions—PSMA-targeted PET/CT appears to aid in the identification of patients with oligometastatic clear cell RCC. If borne out in future studies, this suggests that PSMA-targeted imaging has the potential to help select candidates for metastasis-directed therapy.

Keywords

Clear cell; Oligometastatic; Renal cell carcinoma; PSMA

Introduction

It is estimated that 20–40% of patients with renal cell carcinoma (RCC) will develop metastatic disease [1]. For patients presenting with a limited number of metastatic sites, complete surgical metastasectomy is associated with improved overall and cancer-specific survival [2, 3]. A major challenge of this approach, however, is accurate characterization of a patient's extent of disease. At the present time, anatomical imaging techniques such as computed tomography (CT) and magnetic resonance imaging (MRI) are limited in their ability to detect metastatic lesions, in particular lesions < 1 cm [4]. Thus, there is a significant need for more sensitive imaging modalities in the management of patients with RCC.

Molecular imaging with positron emission tomography (PET) offers a potentially more sensitive alternative to conventional imaging. Despite the specificity implied by its name, prostate-specific membrane antigen (PSMA) is a cancer-associated protein that is expressed in the neovasculature of a number of solid tumors, including the clear cell subtype of RCC [5–7]. In light of this, there has been growing interest in using PSMA-targeted PET imaging in patients with metastatic clear cell RCC. We and others have preliminarily shown that PSMA-targeted PET imaging may lead to improved detection of small volume sites of disease in patients with metastatic clear cell RCC, while maintaining excellent specificity [8–13].

In this study, we explored the utility of PSMA-targeted ^{18}F-DCFPyL PET/CT in the evaluation of patients with presumed oligometastatic clear cell RCC. We hypothesized that a proportion of patients who were diagnosed with oligometastatic disease on the basis of conventional anatomical imaging studies would be found to have more extensive disease on PET/CT imaging, potentially impacting their disease management.

Methods

Study design and participants

The study cohort was comprised of a subset of patients who were originally enrolled in a prospective study designed to broadly investigate the utility of ^{18}F-DCFPyL PET/CT across a range of RCC stages and histologies (ClinicalTrials.gov identifier NCT02687139). The study protocol was approved by the Institutional Review Board of Johns Hopkins Medicine and all patients provided informed consent prior to enrollment. We have previously reported on the subset of patients enrolled in this study with non-clear cell RCC [14]. The present analysis was limited to patients with oligometastatic clear cell RCC. Given that there is no

consensus on the definition of the oligometastatic state for clear cell RCC in the literature, we used a conservative definition of ≤ 3 metastatic lesions on conventional imaging. Patients who had their primary tumor in place were included in the present analysis, while those who had previously received systemic therapy were excluded.

Imaging

All patients were diagnosed with oligometastatic clear cell RCC based on standard of care conventional cross-sectional imaging with CT of the chest, abdomen, and pelvis or MRI of the abdomen and pelvis with CT of the chest. Additional imaging of the brain was performed as indicated based on clinical symptoms. Following study enrollment, patients underwent an ^{18}F-DCFPyL PET/CT. ^{18}F-DCFPyL was synthesized at our institution as previously described [15]. Patients fasted for 4–6 h prior to intravenous injection of approximately 333 MBq (9 mCi) of ^{18}F-DCFPyL. One hour after injection, patients were asked to void and a whole-body PET/CT was performed from the mid-thighs to the vertex of the skull.

Analysis

^{18}F-DCFPyL PET/CT images were reviewed by a single radiologist (S.P.R.) with 5 years of experience in PSMA-targeted imaging. The location, size, and the maximum lean body mass-corrected standardized uptake value (SUV_{max}) of each detected lesion was recorded. A lesion was considered positive on ^{18}F-DCFPyL PET if there was focal radiotracer uptake above background, after taking into consideration the known pitfalls of PSMA-targeted PET imaging [16]. The detection rate of ^{18}F-DCFPyL PET/CT was then compared to that of conventional imaging. The total number of unique lesions detected on either modality form the denominator for the calculation of the detection rates.

Results

Between August 2015 and August 2017, 37 patients with RCC were enrolled in our prospective study. Of these patients, 14 (37.8%) had oligometastatic clear cell RCC and no prior history of treatment with systemic therapy. The median age of patients included in this study was 59 years (range 34–76) and 9 (64.3%) were male. The median time from diagnosis to metastasis was 7.5 months (range 0–164.5). Based on the International Metastatic RCC Database Consortium prognostic model definitions [17], 7 (50.0%) patients had favorable risk disease, 6 (42.9%) had intermediate risk disease, and 1 (7.1%) had poor risk disease. Additional characteristics of the study cohort are listed in Table 1.

Patients underwent ^{18}F-DCFPyL PET/CT at a median of 20.5 days (range 1–74 days) following conventional imaging. Table 2 lists the sites of disease detected with either conventional imaging or ^{18}F-DCFPyL PET/CT, with lesions visible on only one imaging modality indicated by italics. A total of 33 sites of metastatic disease were identified on conventional imaging and ^{18}F-DCFPyL PET/CT (Example case in Fig. 1). Conventional imaging revealed that patients had a total of 21 metastatic lesions (median 1, range 1–3, per patient) and 3 primary tumors. In contrast, ^{18}F-DCFPyL PET/CT detected a total of 29 sites of abnormal radiotracer uptake consistent with sites of metastatic disease (median

1.5, range 0–6, per patient) and 3 primary tumors. Of the 21 metastatic lesions detected on conventional imaging, 17 (81.0%) had radiotracer uptake. Additionally, all 3 (100%) primary tumors had radiotracer uptake. The median SUV_{max} for metastatic sites was 2.7 (range 0.9–38.5) and the median SUV_{max} for primary tumors was 9.6 (range 7.3–15.8). The detection rate of conventional imaging for identifying sites of metastatic disease and any sites of disease was 63.4%, and 66.7%, respectively. The detection rate of ^{18}F-DCFPyL PET/CT for identifying sites of metastatic disease and any sites of disease was 87.9% and 88.9%, respectively. In 4 (28.6%) patients, a total of 12 more lesions were identified on ^{18}F-DCFPyL PET/CT than conventional imaging (Example case in Fig. 2). Notably, 3 (21.4%) patients were no longer considered oligometastatic due to the presence of more widespread disease detected on ^{18}F-DCFPyL PET/CT (Table 2).

Discussion

In this study, we evaluated the clinical utility of PSMA-targeted ^{18}F-DCFPyL PET/CT in patients with presumed oligometastatic clear cell RCC on the basis of conventional anatomical imaging. We found that ^{18}F-DCFPyL PET/CT had a high detection rate for metastatic lesions, leading to the identification of a greater number of sites of metastatic disease than conventional imaging. Most importantly, with these additional lesions, over 20% of patients in the cohort were no longer considered oligometastatic.

The findings of this study are consistent with prior observations on the diagnostic performance and utility of PSMA-targeted imaging of patients with clear cell RCC. In an earlier series of 5 patients with metastatic clear cell RCC, we observed that nearly all sites of disease on conventional were identified on ^{18}F-DCFPyL PET/CT, with overall more lesions detected using this modality (94.7% versus 78.9% for conventional imaging) [10]. Additionally, in a phase I clinical trial of 10 patients, Rhee et al. reported a sensitivity of 92.11% with ^{68}Ga-PSMA-11 PET/CT versus 68.6% with conventional imaging [13].

The apparent superior detection rate of PSMA-targeted imaging has important implications for patient management. According to current guidelines, patients with oligometastatic RCC should be considered for metastasis-directed therapy with surgery and/or tumor ablation, while those with more widespread disease should be treated with systematic therapy [18, 19]. Metastasis-directed therapy offers patients with oligometastatic RCC an opportunity for long-term disease-free intervals without the toxicity of current systemic therapies. A recent systematic review showed that complete metastasectomy was associated with median overall survival rates ranging from 36.5 to 142 months versus 8.4 to 27 months in patients that underwent an incomplete or no metastasectomy [3]. In our cohort, 21.4% of patients who met a stringent definition of oligometastatic disease would have no longer been considered appropriate candidates for metastasis-directed therapy. Additionally, in 1 patient who still met the criteria for oligometastatic disease, new sites of disease were revealed on ^{18}F-DCFPyL PET/CT that would not have been addressed had treatment been delivered on the basis of conventional imaging. Accordingly, PSMA-targeted PET/CT appears to have the potential to aid in determining not only who should undergo metastasectomy, but also ensuring more complete treatment in those meeting the definition of oligometastatic disease.

Rhee et al. demonstrated this principle in 2 patients in whom the surgical template was extended based on PSMA PET/CT findings, enabling complete metastasectomy [13].

Interestingly, four patients (Patients 1, 2, 3, and 10) had metastases seen on conventional imaging, but not ^{18}F-DCF-PyL PET/CT. Two possibilities for this phenomenon should be considered. First, PSMA has previously been shown to be expressed at lower levels in clear cell RCC than prostate cancer—a malignancy which is widely imaged with PSMA-targeted imaging and is accepted as having imperfect sensitivity [20]. Thus, it is likely that some sites of RCC lack sufficient PSMA expression for detection by ^{18}F-DCFPyL PET/CT. A second possibility for our observation is that sites characterized as metastases on conventional imaging were not actually metastases. It is well documented that contrast-enhanced CT can lead to the detection of false positives in patients with metastatic RCC. For instance, Rhee et al. found CT had a specificity of only 88.46% (95% CI 76–95%) for identifying metastatic sites [13].

In light of the shortcomings of currently available anatomical imaging techniques, the collective body of data in support of PSMA-targeted PET imaging of RCC is quite encouraging. This is in contrast to the literature on 2-deoxy-2-(18F)fluoro-D-glucose PET, which is widely considered to be unsuitable for imaging renal cancers [18]. Another class of molecular imaging agents that have shown promise in imaging RCC includes radiotracers that target the transmembrane protein carbonic anhydrase IX (CAIX). CAIX maintains extracellular pH balance and is overexpressed after loss of von Hippel–Lindau tumor suppressor gene, a defining event in over 95% of cases of clear cell RCC [21]. Most notable in this class of agents is the chimeric monoclonal antibody targeting CAIX known as girentuximab (also known as G250). In human trials, this radiotracer has shown excellent performance characteristics for imaging metastatic and primary RCC [22, 23]. The relative performance characteristics of CAIX- and PSMA-targeted PET imaging is unknown at this time, as no head-to-heard studies have been performed.

Our study is not without limitations. First, this study is comprised of a small number of patients. Another limitation of our study, and the literature on oligometastatic RCC in general, is the lack of a standardized definition for the oligometastatic state. We did, however, employ a conservative definition of ≤ 3 metastatic sites and one would expect that with an increasing number of allowable sites on conventional imaging a greater proportion of patients would have been found to harbor more extensive disease on PET/CT imaging. Thus, the utility for confirming the diagnosis of oligometastatic RCC is likely understated in our study. Perhaps the greatest limitation of our study is the lack of pathological confirmation that areas of ^{18}F-DCFPyL uptake were indeed sites of metastatic RCC. We have, however, previously shown in a rapid autopsy study the exceptional specificity of the radiotracer [12]. Additionally, Rhee et al. showed that over 97% of PSMA-positive lesions that were biopsied were positive for RCC [13].

Conclusion

This study demonstrates a potential role for PSMA-targeted ^{18}F-DCFPyL PET/CT in patients with presumed oligometastatic clear cell RCC. This molecular imaging test detected

a number of lesions not seen on conventional imaging, and thus offers the potential to impact patient care by enabling more precise delivery of metastasis-directed therapies. Larger studies with follow-up are needed to assess the clinical impact in such patients.

References

1. Psutka SP, Master VA. Role of metastasis-directed treatment in kidney cancer. Cancer. 2018;124(18):3641–55. [PubMed: 29689599]
2. Dabestani S, Marconi L, Hofmann F, et al. Local treatments for metastases of renal cell carcinoma: a systematic review. Lancet Oncol. 2014;15(12):e549–561. [PubMed: 25439697]
3. Zaid HB, Parker WP, Safdar NS, et al. Outcomes following complete surgical metastasectomy for patients with metastatic renal cell carcinoma: a systematic review and meta-analysis. J Urol. 2017;197(1):44–9. [PubMed: 27473875]
4. Brufau BP, Cerqueda CS, Villalba LB, Izquierdo RS, Gonzalez BM, Molina CN. Metastatic renal cell carcinoma: radiologic findings and assessment of response to targeted antiangiogenic therapy by using multidetector CT. Radiographics. 2013;33(6):1691–716. [PubMed: 24108558]
5. Chang SS, Reuter VE, Heston WDW, Bander NH, Grauer LS, Gaudin PB. Five different anti-prostate-specific membrane antigen (PSMA) antibodies confirm PSMA expression in tumor-associated neovasculature. Cancer Res. 1999;59(13):3192–8. [PubMed: 10397265]
6. Chang SS, O'Keefe DS, Bacich DJ, Reuter VE, Heston WDW, Gaudin PB. Prostate-specific membrane antigen is produced in tumor-associated neovasculature. Clin Cancer Res. 1999;5(10):2674–81. [PubMed: 10537328]
7. Chang SS, Gaudin PB, Reuter VE, O'Keefe DS, Bacich DJ, Heston WDW. Prostate-specific membrane antigen: much more than a prostate cancer marker. Mol Urol. 1999;3(3):313–9. [PubMed: 10851338]
8. Chang SS, Reuter VE, Heston WD, Gaudin PB. Metastatic renal cell carcinoma neovasculature expresses prostate-specific membrane antigen. Urology. 2001;57(4):801–5. [PubMed: 11306418]
9. Rowe SP, Gorin MA, Hammers HJ, Pomper MG, Allaf ME, Javadi MS. Detection of ^{18}F-FDG PET/ct occult lesions with ^{18}F-DCF-PyL PET/CT in a patient with metastatic renal cell carcinoma. Clin Nucl Med. 2016;41(1):83–5. [PubMed: 26402128]
10. Rowe SP, Gorin MA, Hammers HJ, et al. Imaging of metastatic clear cell renal cell carcinoma with PSMA-targeted ^{18}F-DCFPyL PET/CT. Ann Nucl Med. 2015;29(10):877–82. [PubMed: 26286635]
11. Sasikumar A, Joy A, Nanabala R, Unni M, Tk P. Complimentary pattern of uptake in 18F-FDG PET/CT and ^{68}Ga-prostate-specific membrane antigen PET/CT in a case of metastatic clear cell renal carcinoma. Clin Nucl Med. 2016;41(12):e517–e519519. [PubMed: 27749421]
12. Gorin MA, Rowe SP, Hooper JE, et al. PSMA-targeted ^{18}F-DCF-PyL PET/CT imaging of clear cell renal cell carcinoma: results from a rapid autopsy. Eur Urol. 2017;71(1):145–6. [PubMed: 27363386]
13. Rhee H, Blazak J, Tham CM, et al. Pilot study: use of gallium-68 PSMA PET for detection of metastatic lesions in patients with renal tumour. EJNMMI Res. 2016;6(1):76. [PubMed: 27771904]
14. Yin Y, Campbell SP, Markowski MC, Pierorazio PM, Pomper MG, Allaf ME, Rowe SP, Gorin MA. Inconsistent detection of sites of metastatic non-clear cell renal cell carcinoma with PSMA-targeted [^{18}F]DCFPyL PET/CT. Mol Imaging Biol. 2019;21(3):567–73. [PubMed: 30218388]
15. Ravert HT, Holt DP, Chen Y, et al. An improved synthesis of the radiolabeled prostate-specific membrane antigen inhibitor, [^{18}F] DCFPyL. J Label Comp Radiopharm. 2016;59(11):439–50.
16. Sheikhbahaei S, Afshar-Oromieh A, Eiber M, et al. Pearls and pitfalls in clinical interpretation of prostate-specific membrane antigen (PSMA)-targeted PET imaging. Eur J Nucl Med Mol Imaging. 2017;44(12):2117–366. [PubMed: 28765998]
17. Heng DYC, Xie WL, Regan MM, et al. Prognostic factors for overall survival in patients with metastatic renal cell carcinoma treated with vascular endothelial growth factor-targeted agents: results from a Largemulticenter study. J Clin Oncol. 2009;27(34):5794–9. [PubMed: 19826129]

18. Network NCC. National Comprehensive Cancer Network. Kidney. Version 2.2019. 2019; https://www.nccn.org/professionals/physician_gls/pdf/kidney.pdf. Accessed 28 Jan 2019.

19. Ljungberg B, Bensalah K, Canfield S, et al. EAU guidelines on renal cell carcinoma: 2014 update. Eur Urol. 2015;67(5):913–24. [PubMed: 25616710]

20. Campbell SP, Baras AS, Ball MW, et al. Low levels of PSMA expression limit the utility of ^{18}F-DCFPyL PET/CT for imaging urothelial carcinoma. Ann Nucl Med. 2018;32(1):69–74. [PubMed: 29067547]

21. Stillebroer AB, Mulders PF, Boerman OC, Oyen WJ, Oosterwijk E. Carbonic anhydrase IX in renal cell carcinoma: implications for prognosis, diagnosis, and therapy. Eur Urol. 2010;58(1):75–83. [PubMed: 20359812]

22. Divgi CR, Uzzo RG, Gatsonis C, et al. Positron emission tomography/computed tomography identification of clear cell renal cell carcinoma: results from the REDECT trial. J Clin Oncol. 2013;31(2):187–94. [PubMed: 23213092]

23. Hekman MCH, Rijpkema M, Aarntzen EH, et al. Positron emission tomography/computed tomography with ^{89}Zr-girentuximab can aid in diagnostic dilemmas of clear cell renal cell carcinoma suspicion. Eur Urol. 2018;74(3):257–60. [PubMed: 29730017]

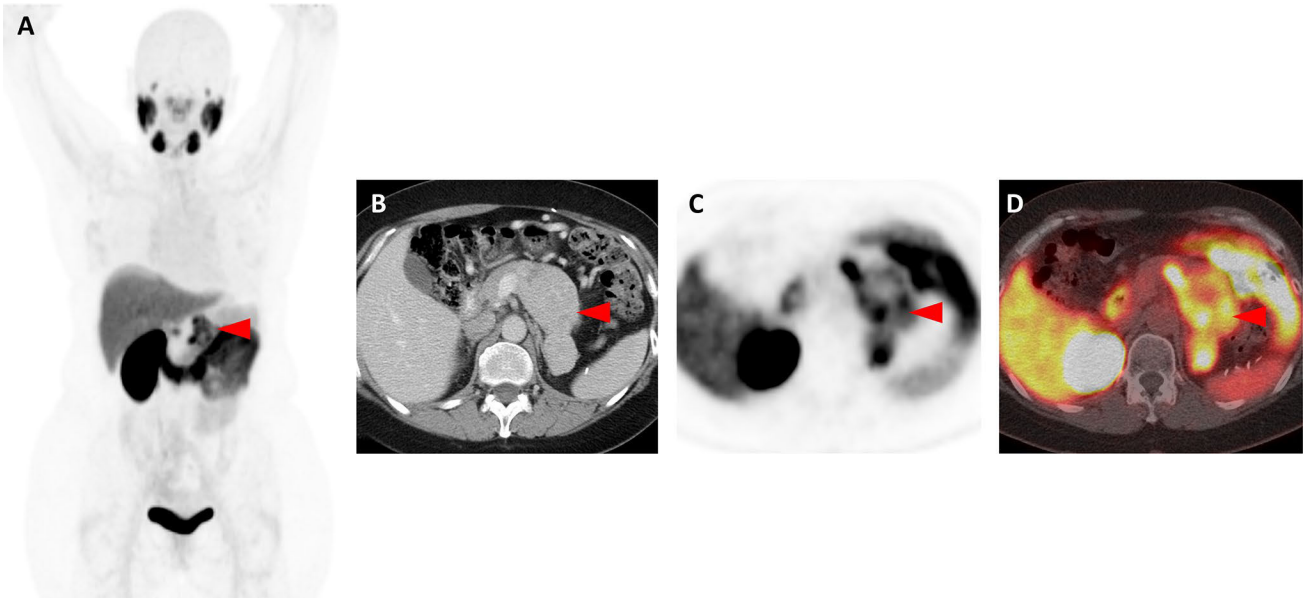

Fig. 1.

Images of a patient with oligometastatic clear cell RCC confirmed with ^{18}F-DCFPyL PET/CT (Patient #12). **a** Whole-body ^{18}F-DCFPyL PET maximum intensity projection image demonstrates a solitary site of abnormal uptake (red arrowhead) in the region of the left nephrectomy bed. **b** Axial, contrast-enhanced, venous-phase CT image demonstrates a recurrence in the left nephrectomy bed with tumor invading and expanding the left renal vein (red arrowhead). **c** Axial ^{18}F-DCFPyL PET and **d** axial ^{18}F-DCFPyL PET/CT images show focal radiotracer uptake in the lesion (red arrowheads)

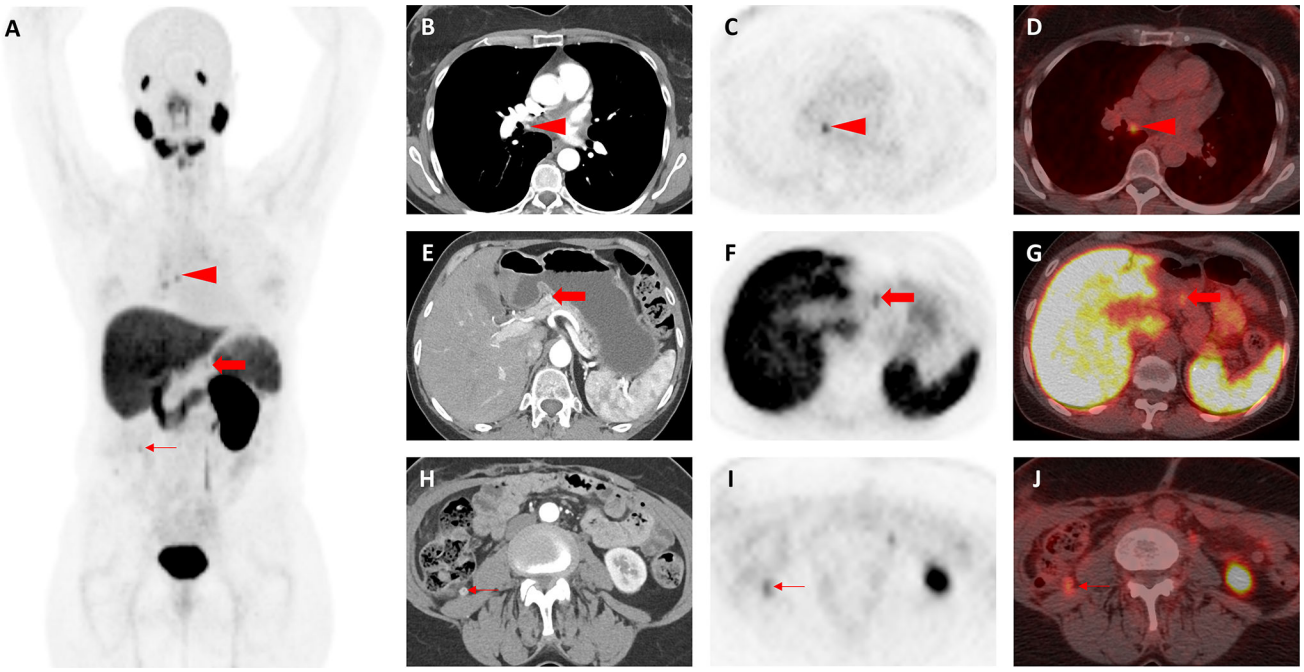

Fig. 2.

Images of a patient with presumed oligometastatic clear cell RCC found to have additional sites of disease on ^{18}F-DCFPyL PET/CT (Patient #2). **a** Whole-body ^{18}F-DCFPyL PET maximum intensity projection image demonstrates multiple foci of abnormal radiotracer uptake, some of which are demonstrated in the accompanying panels (red arrowhead, red arrow, and thin red arrow). **b** Axial, contrast-enhanced, arterial-phase CT image demonstrates subtle arterial enhancement in a small subcarinal lymph node (red arrowhead) that was not initially appreciated prior to PET imaging. **c** Axial ^{18}F-DCFPyL PET and **d** axial ^{18}F-DCFPyL PET/CT images show focal radiotracer uptake in the subcarinal lymph node (red arrowheads), strongly suggesting this is a site of metastatic disease. **e** Axial, contrast-enhanced, arterial-phase CT image demonstrates subtle abnormal enhancement in the neck of the pancreas (red arrow) that was also not appreciated prior to PET imaging. **f** Axial ^{18}F-DCFPyL PET and **g** axial ^{18}F-DCFPyL PET/CT images confirm radiotracer uptake at the same site in the pancreas (red arrows), most compatible with this representing an additional site of metastatic disease. **h** Axial, contrast-enhanced, arterial-phase CT image showing an enhancing nodule in the right paracolic gutter (thin red arrow), compatible with a site of metastatic disease and the original finding that had prompted PET imaging. At the time of the CT, this was thought to be the only site of disease. **i** Axial ^{18}F-DCFPyL PET and **j** axial ^{18}F-DCFPyL PET/CT images demonstrate focal radiotracer uptake in the right paracolic gutter lesion (thin red arrows)

Table 1

Detailed characteristics of the study participants

Patient #	Age	Sex	Race	TNM stage at diagnosis	Time from diagnosis to metastasis (months)	Prior metastasectomy (sites)	Prognostic Risk Group
1	55	F	W	T3aN1M1	0	Lung	Intermediate
2	61	F	W	T3aN1M0	0	N/A	Intermediate
3	47	M	W	T3aN0M1	0	N/A	Favorable
4	58	M	W	T3aN0M1	0	Soft tissue mass	Intermediate
5	40	F	W	T3aN0M1	0	Gamma knife to brain	Intermediate
6	34	M	W	T2aN0M1	0	Radiation to bone	Poor
7	59	M	O	T3aN0M0	51.3	N/A	Favorable
8	74	M	W	T1aN0M0	75.2	Adrenal	Favorable
9	61	M	W	T1bN0M0	20.6	Lung	Favorable
10	62	M	W	T1aN1M0	0	N/A	Intermediate
11	71	M	B	T2aN0M0	15.0	N/A	Favorable
12	58	M	W	T2aN0M0	90.6	N/A	Favorable
13	76	M	W	T1aN0M0	164.5	N/A	Intermediate
14	59	F	W	T3aN0M0	46.0	N/A	Favorable

F female, *M* male, *W* white, *B* black, *O* other

Table 2

Sites of clear cell RCC detected on conventional imaging and PSMA-targeted ^{18}F-DCFPyL PET/CT

Patient #	Number of metastatic sites on conventional imaging[a]	Sites of disease on conventional imaging	Number of metastatic sites on PET/CT[a]	Sites of disease on PET/CT (SUV_{max})	Time between conventional imaging and PET/CT (days)	Continue to be oligometastatic?
1	1	*Adrenal gland*	0	N/A	24	Yes
2	1	*Retroperitoneal lymph node*	6	*Subcarinal lymph node* (3.5 and 3.3), *pancreas* (4.2 and 2.8), *Paracolic gutter* (2.6, 1.8)	13	No
3	1	*Mediastinum,* Primary kidney	0	Primary kidney (9.6)	6	Yes
4	2	Lung, primary kidney	3	Lung (38.5 and 1.3), *bone* (3.9), primary kidney (15.8)	43	Yes
5	2	Breast, brain	2	Breast (10.6), brain (2.5)	25	Yes
6	2	Bone	4	*Bone* (2.08, 2.47, 2.33, 2.67)	43	No
7	2	Pancreas, Retroperitoneal lymph node	2	Pancreas (2.9), retroperitoneal lymph node (3.6)	25	Yes
8	1	Adrenal gland	1	Adrenal gland (N/A[b])	3	Yes
9	2	Pancreas, contralateral kidney	5	Pancreas (4.6), contralateral kidney (5.2), *lung* (0.9), *retroperitoneal lymph node* (2.7), *bone* (1.8)	61	No
10	1	*Retroperitoneal lymph node*, primary kidney	0	Primary kidney (7.3)	7	Yes
11	1	Adrenal gland	1	Adrenal gland (2.7)	74	Yes
12	1	Renal fossa	1	Renal fossa (9.4)	7	Yes
13	1	Retroperitoneal lymph node	1	Retroperitoneal lymph node (8.2)	17	Yes
14	3	Retroperitoneal lymph node, adrenal gland	3	Retroperitoneal lymph node (2.2), adrenal gland (1.9, 2.2)	1	Yes

Lesions visible on only one imaging modality indicated by italics

[a] Primary tumors of the kidney are not included in the total number of metastatic sites

[b] Lesion was too close to liver to accurately obtain SUV_{max}